archives
of thermodynamics
Vol. **36**(2015), No. 1, 125–137
DOI: 10.1515/aoter-2015-0009

Computer modeling of a convective steam superheater

MARCIN TROJAN[1]

Cracow University of Technology, Institute of Thermal Power Engineering, Faculty of Mechanical Engineering, Jana Pawła II 37, 31-864 Cracow, Poland

Abstract Superheater is for generating superheated steam from the saturated steam from the evaporator outlet. In the case of pulverized coal fired boiler, a relatively small amount of ash causes problems with ash fouling on the heating surfaces, including the superheaters. In the convection pass of the boiler, the flue gas temperature is lower and ash deposits can be loose or sintered. Ash fouling not only reduces heat transfer from the flue gas to the steam, but also is the cause of a higher pressure drop on the flue gas flow path. In the case the pressure drop is greater than the power consumed by the fan increases. If the superheater surfaces are covered with ash than the steam temperature at the outlet of the superheater stages falls, and the flow rates of the water injected into attemperator should be reduced. There is also an increase in flue gas temperature after the different stages of the superheater. Consequently, this leads to a reduction in boiler efficiency. The paper presents the results of computational fluid dynamics simulations of the first stage superheater of both the boiler OP-210M using the commercial software. The temperature distributions of the steam and flue gas along the way they flow together with temperature of the tube walls and temperature of the ash deposits will be determined. The calculated steam temperature is compared with measurement results. Knowledge of these temperatures is of great practical importance because it allows to choose the grade of steel for a given superheater stage. Using the developed model of the superheater to determine its degree of ash fouling in the on-line mode one can control the activation frequency of steam sootblowers.

Keywords: Superheater; Steam boiler; CFD modeling; Ash fouling

[1]E-mail: trojan_marcin@interia.pl

Nomenclature

d	–	diameter, mm
g	–	wall thickness, mm
h	–	specific enthalpy, J/kg
k	–	turbulence kinetic energy
$\dot{m}$	–	mass flow rate, kg/s
p	–	pressure, Pa
T	–	temperature, K
t	–	time, s
$\bar{T}$	–	mean temperature, K
$\dot{Q}$	–	heat flux
$\mathbf{U}$	–	fluid velocity vector

Greek symbols

ε	–	dissipation rate of kinetic energy
λ	–	heat conductivity coefficient, W/(m K)
ρ	–	fluid density, kg/m^3
τ	–	stress tensor

Subscripts

a	–	ash
g	–	gas
i, j	–	Einstein Summation indices
in	–	inlet
out	–	outlet
s	–	steam
T	–	temperature, K
w	–	wall

1 Introduction

Superheaters are tubular cross-flow heat exchangers prone to ash fouling [1,2]. However, they differ substantially from other heat exchangers operating in moderate temperatures. Their characteristic features are the complicated flow arrangement and the high temperature of steam and flue gases (Fig. 1). Because the specific heat of the water steam strongly depends on pressure and temperature, conventional method for heat exchanger calculations, such as the number of transfer units (NTU) method or the method based on the mean logarithmic temperature difference between the fluids, are not appropriate for superheaters [3–5].

It is very difficult to design the boiler superheater correctly. This results, on one hand, from the complexity of the radiation heat transfer in the case of flue gases with a high content of solid ash particles, and on the other

hand – from the fouling of heating surfaces by slag and ash [6–9]. Slag and ash deposition processes are hard to evaluate, at the design phase as well as during the boiler operation. For that reason, the proper size of superheaters is adjusted only after the boiler operation starts. If the temperature of superheated steam at the analyzed superheater stage outlet is higher than the design value, the surface area of this stage has to be decreased. Similarly, if the steam outlet temperature is below the desired value, the surface area is increased.

About 40% of all boiler failures are caused by damage to steam superheaters due to the overheating of the material [10]. For this reason, steam superheaters are modelled mathematically or monitored to avoid overheating of tubes.

The paper presents the results of computational fluid dynamics (CFD) simulations of the first stage superheater of the boiler OP-210M using commercial high-performance general purpose fluid dynamics software.

2 Mass, momentum and energy conservation equations and the model of turbulence

The basis for the modeling of thermal and flow processes are the equations of mass, momentum and energy conservation of the following form [11]:

- mass conservation equation

$$\frac{\partial \rho}{\partial t} + \nabla \cdot (\rho \mathbf{U}) = 0 \,, \tag{1}$$

- momentum conservation equation

$$\frac{\partial (\rho \mathbf{U})}{\partial t} + \nabla \cdot (\rho \mathbf{U} \otimes \mathbf{U}) = -\nabla p + \nabla \cdot \tau + \mathbf{S_M} \,, \tag{2}$$

- energy conservation equation

$$\frac{\partial (\rho h)}{\partial t} - \frac{\partial p}{\partial t} + \nabla \cdot (\rho \, \mathbf{U} \, h) = \nabla \cdot (\lambda \nabla T) + \mathbf{U} \cdot \nabla p + \tau : \nabla \mathbf{U} + S_E \,, \tag{3}$$

where: $\mathbf{S_M}$ – momentum source unit power, $\mathrm{kg}/(\mathrm{m}^2\,\mathrm{s}^2)$, and S_E – continuous energy source unit power, $\mathrm{kg}/(\mathrm{m}\,\mathrm{s}^3)$.

The stress tensor τ, being the function of the strain rate, is defined as [11]:

$$\tau = \mu \left(\nabla \mathbf{U} + (\nabla \mathbf{U})^T - \frac{2}{3} \delta \nabla \cdot \mathbf{U} \right) , \tag{4}$$

where δ is the unit matrix, and T denotes the transpose.

The turbulent flow of flue gases and steam in the superheater tubes was simulated by means of the k-ε turbulence model [12], focused on mechanisms that have an impact on the turbulence kinetic energy. It is a two-dimensional model introducing two additional equations: the turbulence kinetic energy, k, equation and the kinetic energy dissipation rate ε.

The following can be written for the turbulence kinetic energy and its dissipation:

$$\frac{\partial (\rho k)}{\partial t} + \frac{\partial (\rho k u_i)}{\partial x_i} = \frac{\partial}{\partial x_j} \left(\frac{\mu_t}{\sigma_k} \frac{\partial k}{\partial x_j} \right) + 2\mu_t E_{ij} E_{ij} - \rho\varepsilon , \tag{5}$$

$$\frac{\partial (\rho \varepsilon)}{\partial t} + \frac{\partial (\rho \varepsilon u_i)}{\partial x_i} = \frac{\partial}{\partial x_j} \left(\frac{\mu_t}{\sigma_\varepsilon} \frac{\partial \varepsilon}{\partial x_j} \right) + C_{1\varepsilon} \frac{\varepsilon}{k} 2\mu_t E_{ij} E_{ij} - C_{2\varepsilon} \rho \frac{\varepsilon^2}{k} , \tag{6}$$

where: u_i – component of velocity in the relevant direction, E_{ij} – strain rate component, μ_t – turbulence dynamic viscosity coefficient

$$\mu_t = \rho C_\mu \frac{k^2}{\varepsilon} . \tag{7}$$

The coefficients in Eqs. (5) – (7) were found empirically and are [13]: $\sigma_k = 1.0$, $\sigma_\varepsilon = 1.3$, $C_{1\varepsilon} = 1.44$, $C_{2\varepsilon} = 1.92$, $C_\mu = 0.09$, respectively.

3 Example of CFD modeling of a convective steam superheater

The CFD simulation was performed for the first stage superheater in the OP-210M boiler using software package ANSYS-CFX, [11]. The first stage of the convective superheater is a mixed-cross-flow heat exchanger with twelve passes [14]. The tubes are arranged in-line. The steam flows through two parallel tubes that create one pass. In the entire superheater steam flows parallel through 148 tubes. The location of the first stage superheater in the boiler is presented in Fig. 1 and the superheater diagram – in Fig. 2. The first stage superheater is made of tubes with an outer diameter $d_z = 42\,\text{mm}$ and the wall thickness $g = 5\,\text{mm}$. The tube material is the Russian steel

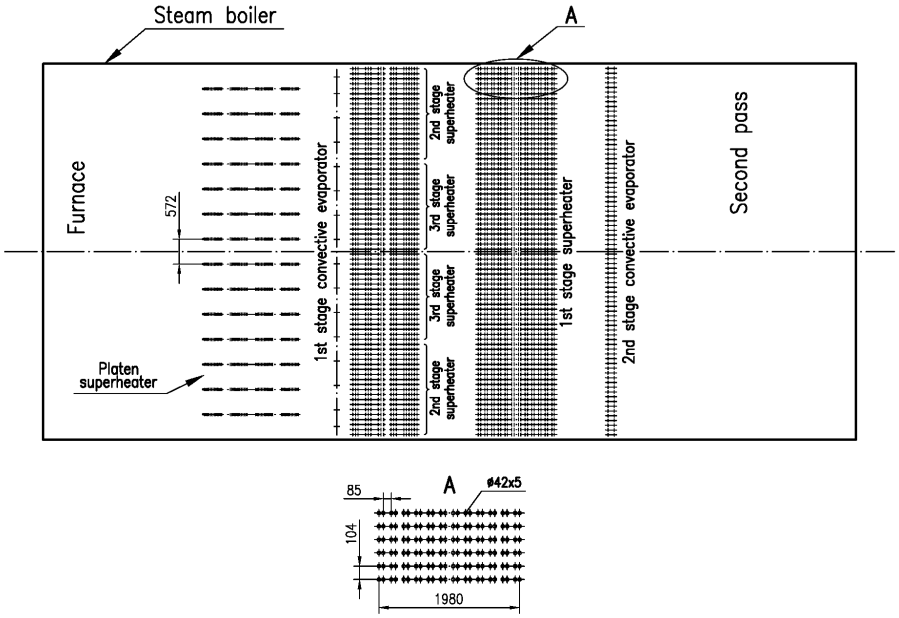

Figure 1: First stage superheater location in the OP-210M boiler.

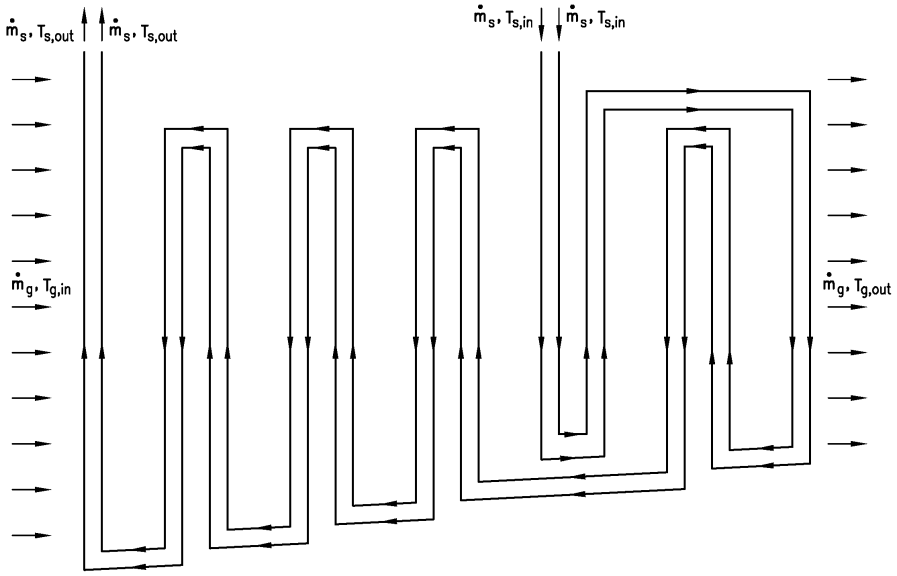

Figure 2: Diagram of the first stage superheater.

20, for which the thermal conductivity coefficient, λ_{st}, was approximated with the following formula:

$$\lambda_{st}(T) = 51.7465 - 0.006704\,T - 0.0000419\,T^2\,. \tag{8}$$

Formula (8) was determined based on experimental data using the TableCurve program, [15].

3.1 Modeled element of the superheater

Numerical calculations were carried out for a repeatable element of the first stage superheater made of one row of the superheater tubes with real dimensions (Fig. 3). A layer of ash deposits with an identical thickness $\delta_a = 1.8\,\mathrm{mm}$ and the same thermal conductivity coefficient $\lambda_a = 0.18\,W/\mathrm{m\,K}$ was assumed on the outer surface of each tube in the row.
The flue gas temperature at the superheater inlet was $T_{g,in} = 1044.65$ K. The mass flow rate of the flue gas in the entire superheater was $\dot{m}_g = 64.5\,\mathrm{kg/s}$, which gives a $\Delta\dot{m}_g = 0.871\,\mathrm{kg/s}$ mass flow rate of flue gase flowing into the repeatable element of the superheater composed of a single tube row. The flue gas was modeled as a mixture of the following components: N_2, CO_2, SO_2, O_2 and H_2O with respective mass contents and properties. The steam temperature at the superheater inlet was $T_{s,in} = 590.35$ K. The steam mass flow rate in the first stage superheater was $\dot{m}_s = 49.5\,\mathrm{kg/s}$, which means that the steam mass flow rate per tube was $\Delta\dot{m}_s = 0.334\,\mathrm{kg/s}$. The properties of superheated steam were defined based on the IAPWS IF97 data.

The mesh for the CFD calculations was created using the HyperMesh 11 program[16]. The constructed model had 7809105 elements. Such a great number of elements results from the fact that the numerical calculations were performed for the first stage superheater real dimensions. Figure 4 presents a fragment of the mesh, taking account of the boundary layer for steam and flue gas.

3.2 Calculation results

The results of CFD calculations are presented below. Based on the CFD analysis, the steam temperature at the superheater outlet, the flue gas temperature distribution after the superheater and the maximum temperature of the tube wall are determined. The knowledge of these quantities is necessary to design the superheater correctly.

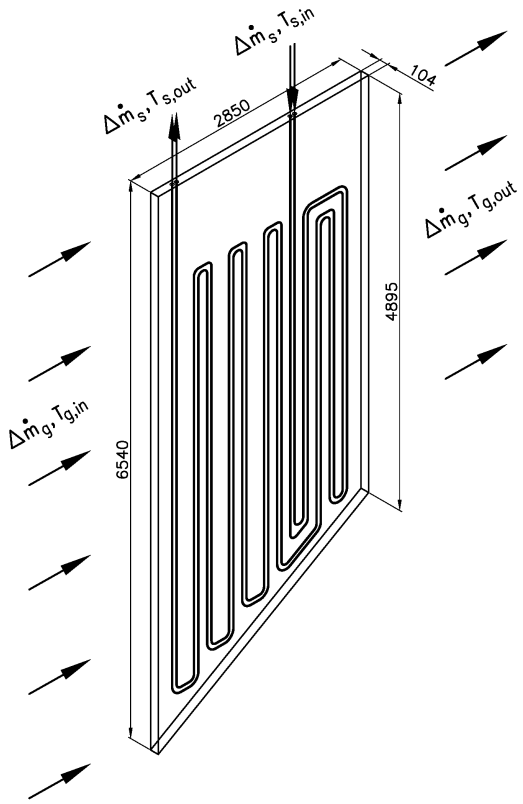

Figure 3: A repeatable fragment of the first stage superheater made of one tube row.

Figure 5 presents the flue gas temperature distribution after the first stage superheater. It can be seen that in the area of the superheater tubes the flue gas temperature falls the most. In the vicinity of the flue gas duct walls, the temperature of flue gas is much higher. The flue gas mean temperature at the outlet of the repeatable element of the first stage superheater for which the calculations were made is $\bar{T}_{g,out} = 881.65$ K.

Figure 6 presents the flue gas temperature distribution in the cross-section in the axis of a single tube row of the first stage superheater (in the centre of the repeatable superheater fragment). It can be seen clearly how the flue gas temperature gets lower as they flow through the superheater. In the superheater tube area, the flue gas-to-steam heat transfer occurs. Figure 7 presents the flue gas temperature distribution in the cross-section made transversely to the flow direction. The cross-section goes through the

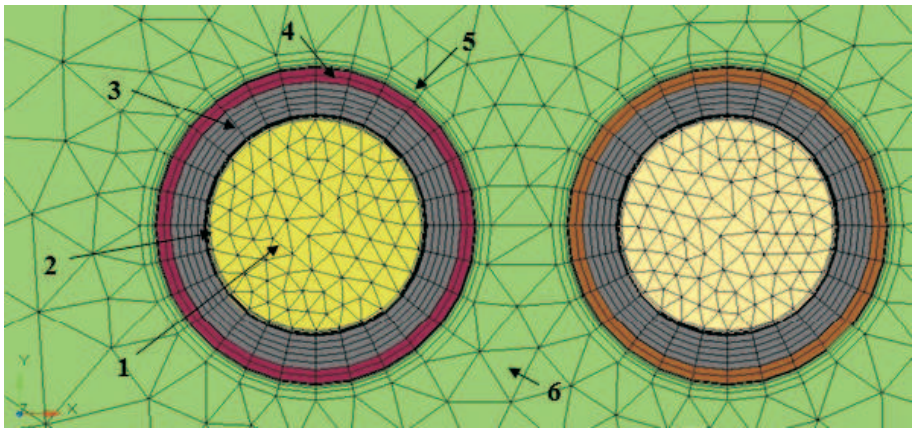

Figure 4: Mesh taking account of the boundary layer for steam and flue gases: 1 – steam, 2 – boundary layer for superheated steam, 3 – tube, 4 – ash deposit layer, 5 – boundary layer for flue gas, 6 – flue gas.

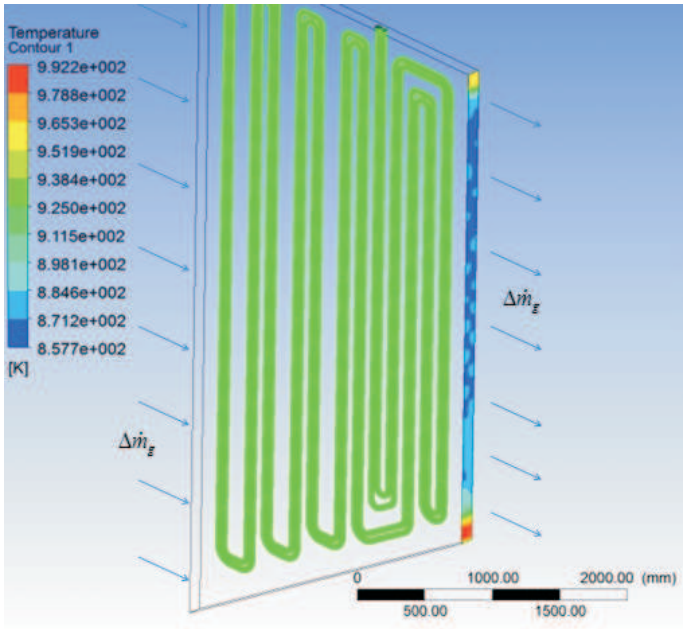

Figure 5: Flue gas temperature distribution at the outlet of the repeatable fragment of the superheater (after the superheater).

centre of the outlet height of the flue gas duct (of the repeatable superheater element). Figure 7 illustrates changes in the flue gas temperature flowing

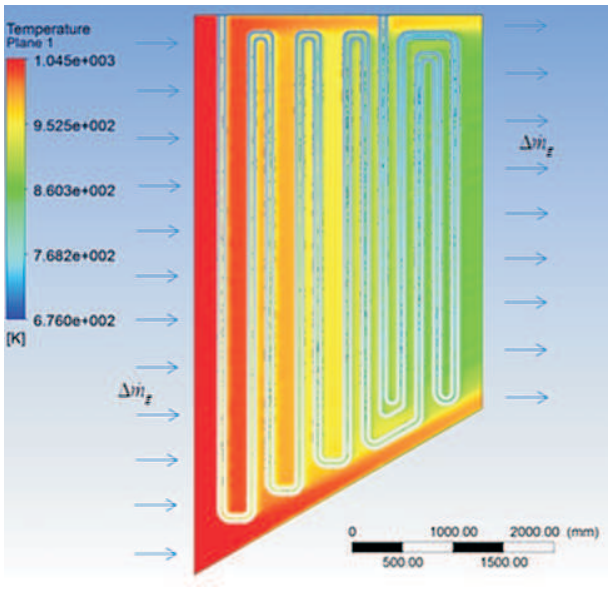

Figure 6: Flue gas temperature distribution in the cross-section going through the centre of the repeatable element of the superheater.

past subsequent tubes of the superheater. It can be seen that the flue gas temperature is much lower close to the tubes, compared to areas more distant from them.

Figure 8 presents the superheated steam temperature distribution at the first stage superheater outlet. It can be seen that a steam boundary layer is formed at a temperature higher than the temperature of steam farther away from the tube wall. The mean temperature of steam at the first stage superheater outlet is $\bar{T}_{s,out} = 656.15$ K.

Figure 9 illustrates changes in the superheater tube wall temperature along the steam flow path. It can be seen that the wall temperature is the lowest at the location where steam flows into the superheater. It then increases gradually to reach highest values in the superheater steam outlet area, i.e. in the area of the highest temperature of flue gas. The maximum temperature of the first tube wall is $T_{w1,\max} = 675.15$ K, whereas the second tube wall maximum temperature amounts to $T_{w1,\max} = 669.45$ K. The knowledge of these temperatures is extremely essential because it allows for the correct selection of the material for the superheater tubes at the design stage.

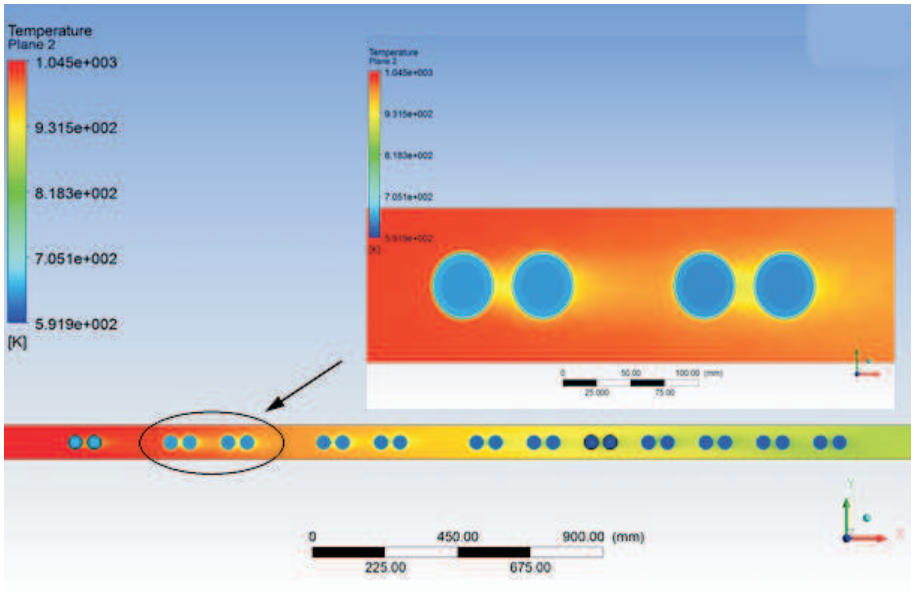

Figure 7: Flue gas temperature distribution within one pass at the horizontal plane passing through the center of the flue gas duct.

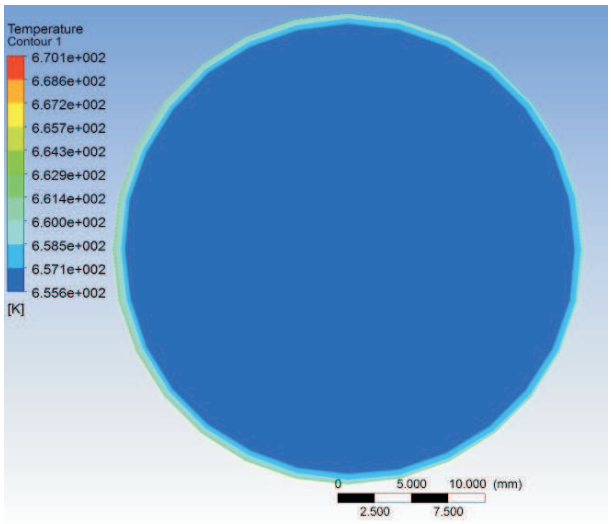

Figure 8: Steam temperature distribution at the first stage superheater outlet.

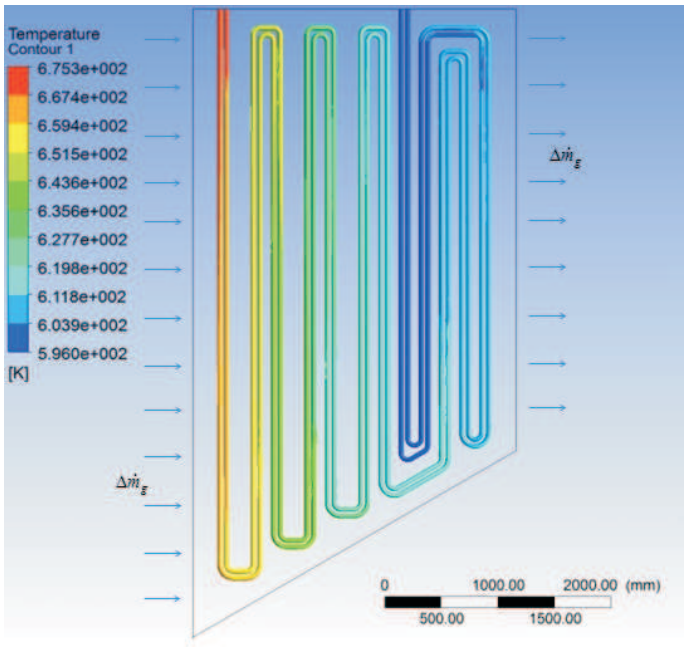

Figure 9: Temperature distribution of the first stage superheater tube walls.

In order to check whether the heat flow transferred from the flue gas to the steam at the analyzed repeatable fragment of the first stage superheater is the same, the heat flux passed from the flue gas and absorbed by the steam was determined. In this way, the correctness of the CFD simulation has been checked. The heat rate values are: $\dot{Q}_g = 176.0$ kW and $\dot{Q}_s = 178.2$ kW for the flue gas side and the steam side, respectively. As it can be seen, the difference between the values is slight, which makes it possible to state that the energy balance was maintained.

In order to investigate the impact of the mesh density on the computation accuracy, calculations were also performed for a model with a denser mesh. As in the previous case, the CFD simulation was carried out for the selected repeatable fragment of the superheater. The computational model consisted of 8490342 elements. The calculations gave the following results:

- the mean temperature of flue gase at the outlet from the repeatable element of the superheater: $\bar{T}_{g,out} = 880.95$ K
- the mean temperature of steam at the first stage superheater outlet: $\bar{T}_{s,out} = 656.75$ K

- the maximum temperature of the first tube wall: $T_{w1,\max} = 675.75$ K
- the maximum temperature of the second tube wall: $T_{w2,\max} = 669.75$ K.

It can be seen that the calculations performed for the two models gave very similar results, which proves that the mesh was selected correctly.

CFD simulation was also conducted for the clean superheater without ash deposits. The steam temperature at the exit of the superheater is about 60 K higher than that for the fouled superheater. This temperature increase in steam temperature was confirmed by calculations which were conducted using a numerical model of the superheater presented in [14] and also by boiler measurements. The flue gas temperature after each row of tubes is lower for the clean superheater, and the tube wall temperatures are higher.

4 Conclusions

The calculations were performed on a model with real dimensions, taking account of the ash deposit layer on the outer surfaces of the first stage superheater tubes. The modelling of the thermal and flow processes in a repeatable fragment of the first stage superheater using the commercial program allowed determination of the local and mean values of:

- flue gas temperature after the first stage superheater,
- steam temperature at the superheater outlet,
- temperatures of the tube walls.

Additionally, the maximum values of temperatures were found for the superheater tube walls. The knowledge of the quantities mentioned above is essential because it makes it possible to design the superheater correctly.

Received 10 December 2014

References

[1] Wessel B., Rüsenberg D., Schlenkert J.U., Thiele I., Karkowski G.: *Betriebserfahrungen mit dem Block Niederaußem K.* VGB PowerTech **11**(2006), 47–51.

[2] Taler J. (Ed.): *Thermal and flow processes in large power boilers. Modelling and monitoring.* PWN, Warsaw 2010.

[3] Hewitt G.F., Shires G.L., Bott T.R.: *Process Heat Transfer.* CRC Press – Begell House, Boca Raton 1994.

[4] Shah R.K., Sekulić D.P.: *Fundamentals of heat exchanger design*. Wiley, Hoboken 2003.

[5] Kakaç S., Liu H.: *Heat Exchangers: Selection, Rating, and Thermal Design*, 2nd Edn., CRC Press – Taylor & Francis Group: Boca Raton 2002.

[6] Lokshin V.A., Peterson D.F., Schwarz A.L.: *Standard Methods of Hydraulic Design for Power Boilers*. Hemisphere Publishing, Washington – New York – London 1998.

[7] Kuznetsov N.W., Mitor W.W., Dubovski I.E., Karasina E.S. (Eds.): *Thermal Calculations of Steam Boilers (Standard Method)*, 2nd Edn., Energia, Moscow 1973.

[8] Lin Z.H.: *Thermo-Hydraulic Design of Fossil-Fuel-Fired Boiler Components* [in:] S. Kakaç (Ed.): *Boilers, Evaporators, and Condensers*. John Wiley & Sons, Hoboken 1991, 363–469.

[9] Taler J., Trojan M., Taler D.: *Monitoring of Ash Fouling and Internal Scale Deposits in Pulverized Coal Fired Boilers*. Nova Science Publishers, New York 2011.

[10] French D.N.: *Metallurgical failures in fossil fired boilers*, 2nd Edn., John Wiley & Sons, New York 1993.

[11] *CFX-ANSYS 15 Theory guide*. ANSYS, Inc. Canonsburg, USA.

[12] Launder B.E., Spalding D.B.: *The numerical computation of turbulent flows*. Comput. Method. Appl. M. **3**(1974), 2, 269–289.

[13] Versteeg H.K., Malalasekera W.: *An Introduction to Computational Fluid Dynamics: The Finite Volume Method*. Pearson Education Limited 2007.

[14] Taler D., Trojan M., Taler J.: *Mathematical modelling of cross-flow tube heat exchangers with the complex flow arrangement*. Heat Transfer Eng. **35**(2014), 11-12, 1334-1343.

[15] *TableCurve 2d*. Systat Software Inc. 2002

[16] *HyperMesh 12.0 - Altair HyperWorks 12.0*. Altair Engineering Inc. 2013.